ENGINEERING RESEARCH INSTITUTE
THE UNIVERSITY OF MICHIGAN
ANN ARBOR

Progress Report No. 4

COMPUTER COMPONENTS DEVELOPMENT

K. E. Monroe

Harvey L. Garner
Project Supervisor

Project 2452

NATIONAL SECURITY AGENCY
SIGNAL CORPS PROCUREMENT OFFICE
CONTRACT NO. DA-49-170-sc-1791
WASHINGTON, D. C.

March 1957

TABLE OF CONTENTS

LIST OF ILLUSTRATIONS

ABSTRACT

This report is an analysis of a pulse amplifier of the type employed in the SEAC computer-gating package. There are two ways of investigating the performance of a given circuit. The first of these is a theoretical analysis of the circuit, and the second is experimentation. The theoretical work, unless grossly inapt assumptions are made, will give the investigator at least an order-of-magnitude feeling for values of circuit parameters and frequencies of operation. In this report linear circuit analysis and a graphical method of analysis are used, and the results are compared with experimental results. Agreement between the theoretical and experimental results is reasonable on the basis of the assumptions made.

OBJECTIVE

The objects of this phase of the computer-components development program are to determine the pulse amplifier-circuit parameters which limit the pulse-repetition rate, to develop theoretical methods of analysis and to use these methods to predict the theoretical limit imposed by presently available components and to experimentally determine the upper limit using available components.

1. THEORETICAL ANALYSIS OF PULSE AMPLIFIERS

1.1 QUALITATIVE DISCUSSION OF A PENTODE, TETRODE, OR CASCODE TRIODE PULSE AMPLIFIER

If the amplifying component is a vacuum tube, then a pulse transformer is required to match the tube to the lower impedance of the gating structure. The tube and transformer then comprise a pulse amplifier. Operation of such a pulse amplifier is best understood by consideration of three different phases of the pulse: the rise, the flat top or duration, and the fall or decay.

1.1.1 The rise.—Initially the pulse amplifier has on its grid a voltage e_{g_1}, which keeps the tube in a low-conduction state. The plate voltage is the supply voltage since there is negligible d-c drop in the transformer. This quiescent point corresponds to point A of Fig. 1. When a pulse is applied by the gating structure, the grid is suddenly raised to the positive value e_{g_2}. Since there is plate-circuit shunt capacitance, the plate voltage cannot change instantly; hence, the plate characteristics are traversed to point B. The tube is now drawing much more current than previously, the capacitance begins to charge, and the plate voltage begins to fall. The plate characteristics are traversed along the e_{g_2} curve towards zero plate volts, and the voltage across the transformer increases. This process continues until the current in the transformer secondary is in equilibrium with the plate current. At the equilibrium point, the capacitance is charged (draws zero current at this instant) and no further increase in transformer voltage will occur. This point is where the line of the load resistance, referred to the primary, intersects the e_{g_2} curve, and it marks the end of the rise-time response of the pulse amplifier. This point is marked C on the figure, and it occurs where the tube is "bottomed." Bottomed operation is desirable since the plate voltage in the bottomed condition changes very little as the tube ages[1]. Hence, the amplitude of the output pulse should remain near the standard value over the useful life of the tube.

1.1.2 The duration.—The rise time is so short that the transformer primary inductance does not have time to begin drawing a great deal of current. However, once the capacitance is charged,

---

1. C.C. Harris, "The 'Hard-Bottoming' Technique in Nuclear Instrumentation," Institute of Radio Engineers, Professional Group on Nuclear Instrumentation, Vol. NS-3, No. 2, March 1956.

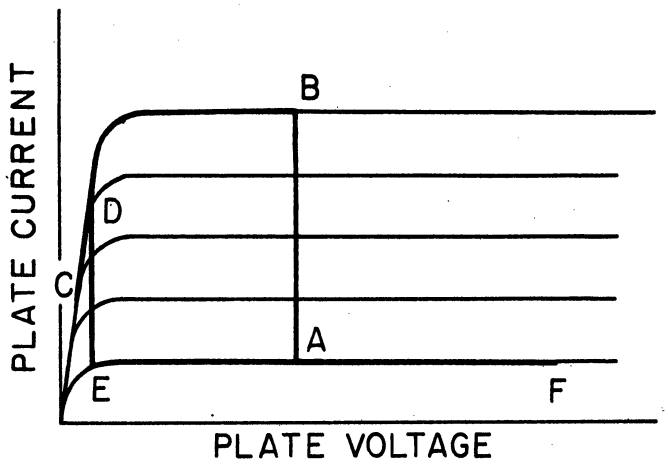

Fig. 1. Pentode operating path.

the transformer has an almost constant voltage impressed and magnetizing current will begin to build up comparatively rapidly. The point of operation on the plate characteristics will move away from point C back up the e_{g_2} curve toward the knee. This means that the plate voltage is increasing, the transformer voltage is falling, and the output pulse is drooping. The magnitude of the droop will depend upon the primary inductance, the pulse duration, and the plate resistance of the tube in the bottomed condition. If the transformer inductance could be made large, then the magnetizing current and output pulse droop could be kept small. However, as will be seen in the next section, the amount of transformer inductance that may be used at a given repetition rate is fixed by factors other than magnetizing current.

1.1.3 The fall—At the end of the pulse, the increased magnetizing current has increased the total tube current up to point D on the curves. At this time, the grid is again switched suddenly to e_{g_1}, and again, because of plate shunt capacitance, the voltage cannot change instantly and the plate characteristics are traversed to point E. At this time we have essentially a parallel RLC circuit with an initial charge on the capacitance and with an initial current in the inductance. The R is the load resistance referred to the primary side of the transformer. As the capacitor discharges, the operating point travels along e_{g_1} to A, at which point a critical damping resistance is switched in and the load resistance is switched out by diodes. The current in the inductance then decays and produces a back voltage out to point F and finally back to point A before the next pulse comes along. Rough sketches of important waveforms during a pulse period are shown in Fig. 2.

In "speeding up" SEAC-type circuitry, an important factor is plate-circuit shunt capacitance. If the transformer is to recover after one pulse before the next one comes along, the resonant frequency of the transformer primary inductance and the plate-circuit shunt capacitance must be equal to or greater than the desired repetition rate[2].

2. R. Denton, W. Brown, and W. Kilmer, Computer Components Development, Report No. 2, January 1957.

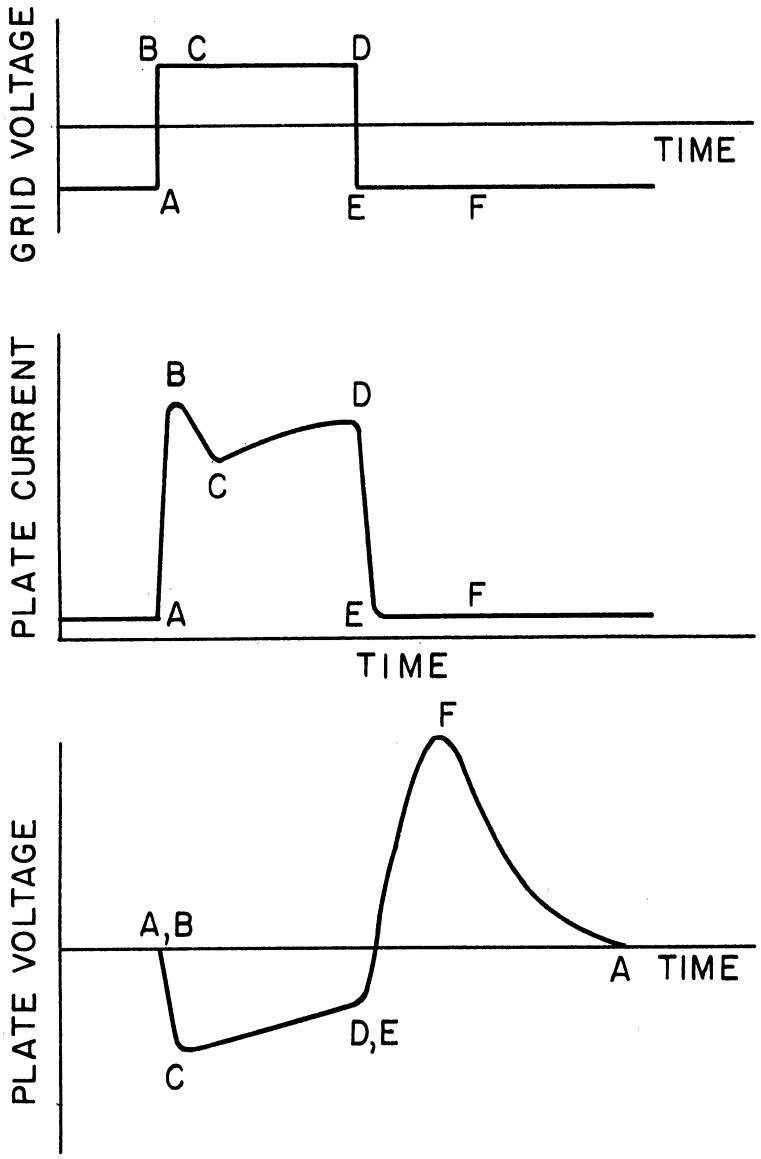

Fig. 2. Pentode waveforms.

This means that the allowable transformer inductance is fixed by the tube and stray capacitances so that the magnetizing current and pulse-top droop which result from this amount of inductance must simply be tolerated. If the inductance is made lower than is necessary to allow sufficiently fast recovery, and/or if the load resistance is made too small, the magnetizing current will carry the path of operation back around the knee of the curve where a very small further increase in magnetizing current will cause the plate voltage to rise quickly to the supply voltage and the load current and voltage to fall to zero before the grid pulse is over. That is, the amplifier will not "hold up" a pulse of the width being amplified. This condition indicates that the limit to which the circuit may be loaded has been exceeded.

The same circuit may be loaded more heavily if the grid is

driven more positive so that the knee to which the magnetizing current must creep is higher. The extent to which this may be carried is limited by either the current or power-dissipation ratings of the tube employed. Usually the plate dissipation is low since high plate current occurs only at low plate voltage and vice versa in this type of amplifier. Consequently, the limit is set by screen dissipation or cathode current, according to which rating is reached first.

1.2 QUALITATIVE DISCUSSION OF A TRIODE PULSE AMPLIFIER

From the considerations similar to the preceding, we see that the path of operation on triode plate characteristics is ABCDEFA, as shown in Fig. 3. The waveforms are sketched in Fig. 4. These waveforms are similar to the pentode case, except that the plate current increases

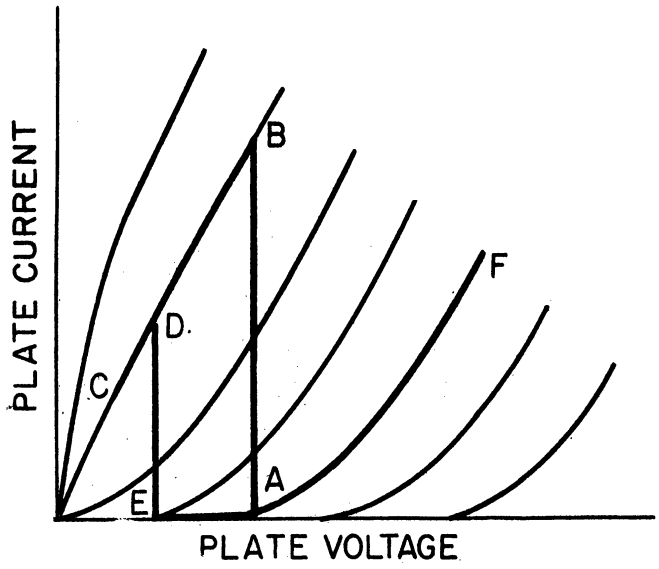

Fig. 3. Triode operating path.

during the transformer backswing where the plate voltage rises above the supply voltage. This additional current may become a significant part of the average plate current, which is undesirable because, in the case of a triode, the tube rating which is likely to be exceeded first is that of average cathode current. The current increase may be eliminated by using a large quiescent bias or possibly by feedback. The first of these would require a large grid swing to drive the tube into heavy conduction, and this is undesirable. Hence, the solution appears to be feedback which would bias the grid more negative as the plate swings positive. This feedback can presumably be derived from the regular package output which is swinging negative at the required time. Further discussion of a triode amplifier is given in section 1.3.1.

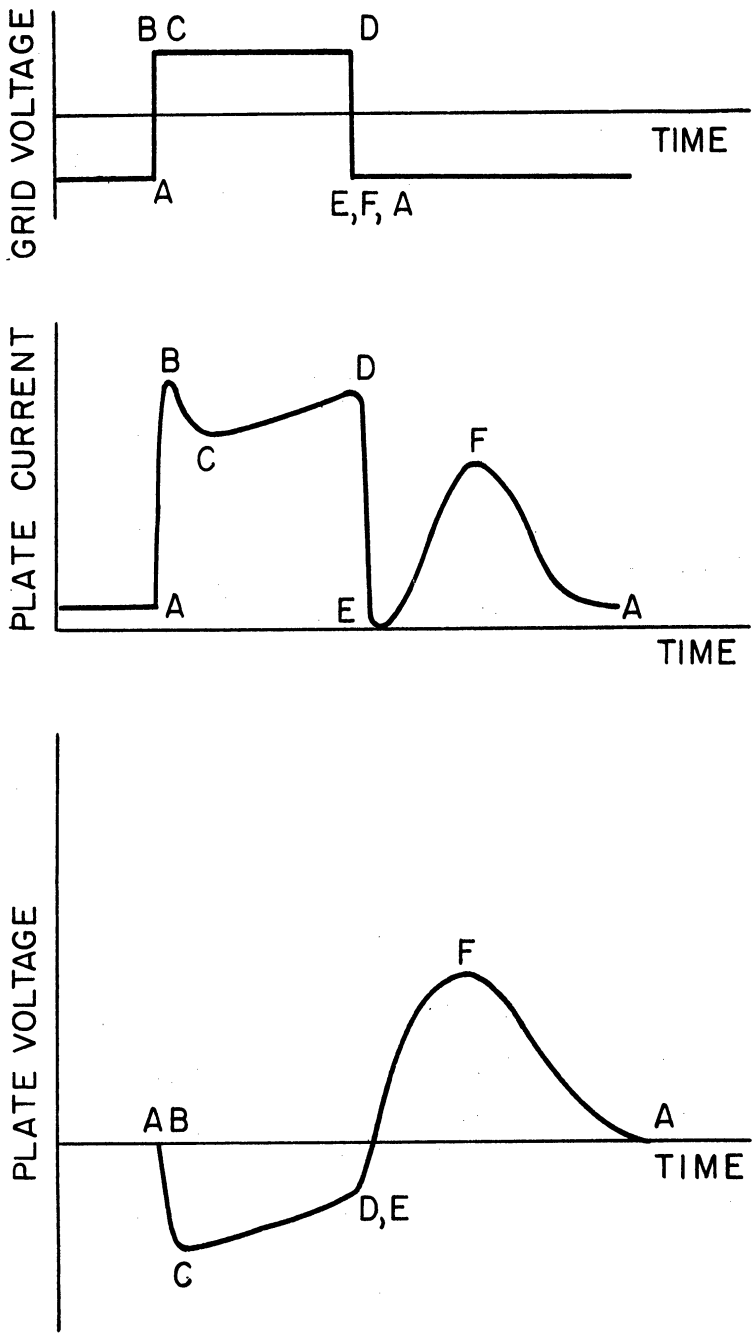

Fig. 4. Triode waveforms.

1.3 LINEAR CIRCUIT ANALYSIS OF POSSIBLE AMPLIFIER CONFIGURATIONS

1.3.1 General discussion.—It is the purpose of this section to develop formulae to be used to estimate the number of gate drives that may be expected from several amplifier configurations. In Appendix B of Computer Components Development, Report No. 2, it is shown that the maximum load current from a tube-transformer pulse amplifier is given by

$$I_{L_{max}} = \frac{23}{140\pi^2} \frac{\Delta I^2}{C_p f E_s} - \frac{35\pi^2}{23} f E_s C_s , \qquad (1)$$

where:
ΔI = pulse-plate current
C_p = primary shunt capacitance
E_s = secondary voltage
C_s = secondary shunt capacitance
f = frequency of operation

If we assume:

(1) that a linear analysis is valid; i.e., that $I = g_m e_g$, where g_m is the tube transconductance and e_g is the grid voltage change,

(2) that one volt of noise clipping is necessary and there is a drop of 2 volts in the diode logic so that $E_s = e_g + 3$, and

(3) that secondary capacitance may be neglected,

then Eq. (1) may be rewritten as

$$I_{L_{max}} = \frac{23}{140\pi^2} \frac{g_m^2 e_g^2}{C_p f (e_g + 3)} . \qquad (2)$$

The current required per gate is calculated by considering the circuit of Fig. 5. A current I_1 is required to charge and discharge the input capacitance of the pulse amplifier; hence, a current of $2I_1$ is required in the "and" pull-up resistor. From noise considerations it is necessary to have a current I_2 flowing in clamp diode D_1. Hence, the input gate current, I_{gate}, is

$$I_{gate} = 2I_1 + I_2 \qquad (3)$$

The current I_1 is given by

$$I_1 = \frac{C_g e_g}{0.1\ T} = 10f\ C_g e_g , \qquad (4)$$

where $T = 1/f$ = pulse repetition period.

The number of gates that may be driven by a gating package is then

$$N = \frac{I_{L_{max}}}{I_{gate}} = \frac{\frac{23}{140\pi^2} \frac{g_m^2 e_g^2}{C_p f (e_g + 3)}}{20 f\ C_g e_g + I_2} . \qquad (5)$$

Eq. (5) applies only as long as none of the ratings of the tube employed are exceeded.

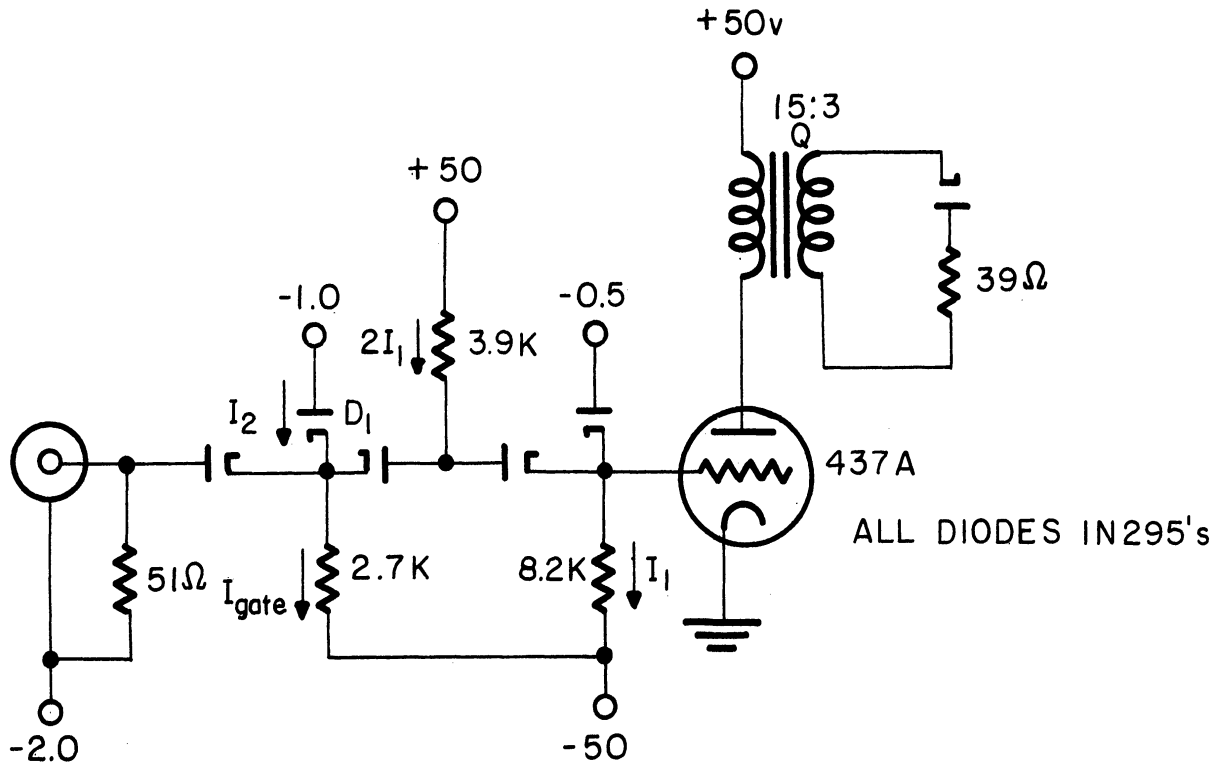

Fig. 5. Triode test circuit.

Within the ratings of the tube employed, Eq. (5) applies to several amplifier configurations provided the proper input and output capacitances and g_m's are used. Capacitances for several configurations are as follows:

(a) If a pentode or tetrode tube is used, the input capacitance may be taken as the capacitance from the control grid to the cathode and to the screen grid plus stray wiring capacitance. The output capacitance is the capacitance from the plate to the cathode and to the screen and suppressor grids plus transformer and stray capacitances. These input and output capacitances, except for the stray components, are ordinarily published by tube manufacturers.

(b) In a triode the Miller Effect capacitance becomes the dominating part of the input capacitance. This capacitance has a transient and a steady-state component. However, as shown in the appendix of this report, the steady-state value is reached in such a short time that the transient may be neglected for operation at frequencies equal to or less than 10 mcps. The input capacitance is then effectively given by

$$C_g = C_{gk} + (1 - A)\, C_{pg} \quad . \qquad (6)$$

Some experimentation has been performed with the 437A triode to illustrate the Miller Effect. The circuit used was the same as that shown in Fig. 5. Results of the experiment are shown in Fig. 6. Fig. 6(a) shows the grid waveform with the plate supply turned off. In this case the capacitance at the grid is just the grid-to-cathode

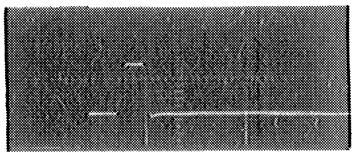

(a) 0.1 μsec/major division
2.0 v/major division

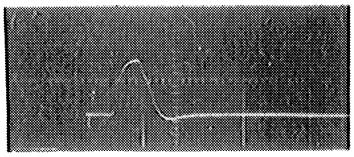

(b) 0.1 μsec/major division
2.0 v/major division

Fig. 6. Waveforms for the triode circuit.

capacitance and the stray capacitance. The gate pull-up and pull-down currents are large enough to charge and discharge the grid capacitance. In Fig. 6(b) the plate supply voltage is turned on, the tube has gain, and the Miller capacitance, which is now present, is large enough to require a comparatively long time to charge and discharge. Presumably it is possible to increase gate currents to the point where they would be able to charge and discharge even the large Miller capacitance in a sufficiently short time. However, such large gate currents would have adverse effects upon the transients in the gating diodes and would require a greater amount of noise clipping. Also, a given triode would be able to drive only a very small number of such high-current gates. It should be possible to drive the input capacitance of the triode by a rather low-power pentode as in Fig. 7, whose small input capacitance could be driven by comparatively low-current gates. The backswing of the pentode's transformer would then tend to keep the triode biased off during its transformer's backswing, thereby reducing the triode average plate current. However, if the rise time of the pulse is not to deteriorate too drastically in this cascade pulse amplifier, then the rise time of the pentode stage and of the triode stage must be the same as for a single-state amplifier. Since rise times of cascaded stages, with rise times T_1, and T_2, add in the square root according to the formula

$$T = \sqrt{(T_1^2 + T_2^2)} \quad , \tag{7}$$

the rise-time requirements on the individual stages become more stringent. In fact, each stage must now rise in only 0.707 of the time that a single-stage pulse amplifier would be allotted.

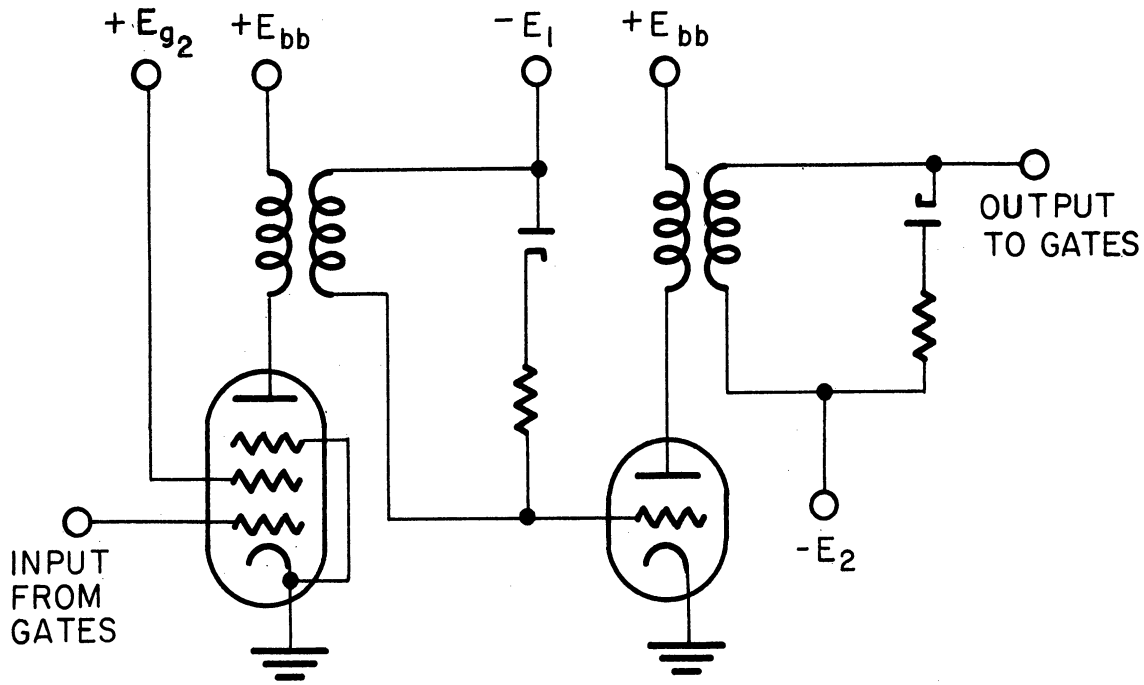

Fig. 7. Pentode-triode pulse amplifier.

(c) If two triodes are used in the cascode configuration, the input and output capacitances will be given by

$$C_P = C_{pg} + \left(1 - \frac{1}{g_m R_L}\right) C_{pk} , \qquad (8)$$

$$C_g = C_{gk} + \left(2 + \frac{R_L}{r_p}\right) C_{gp} \qquad (9)$$

as has been pointed out in the Phase I report.

1.3.2 Predicted gate drives for particular tubes and configurations.

1.3.2.1 436A Tetrode.

The current I_2 of Eq. (3) has been determined experimentally to be about 4 ma. Allowing 5 pF for grid-circuit stray capacitance and a voltage gain of 40, the input capacitance for the 436A is calculated to be 23 pF. The output capacitance with the transformer in place was calculated from the undamped transformer ringing frequency to be about 10 pF. The transconductance is 30 millimhos. Hence,

Eq. (5) may be rewritten as

$$N = \frac{23}{140\pi^2} \frac{(30)^2 (10^{-6}) e_g^2}{f (e_g + 3) 10^{-11}} \frac{1}{20(23)(10^{-12}) f e_g + 4 \times 10^{-3}} . \quad (10)$$

This equation is plotted as a function of frequency with grid swing as a parameter in Fig. 8(a).

1.3.2.2 Cascode 437A.

Again assuming a voltage gain of 40, the input capacitance of 437A's in cascode is calculated to be 27.5 pF. The output capacitance is about 10 pF and the transconductance is 45 millimhos, so that Eq. (5) is evaluated to be

$$N = \frac{23}{140\pi^2} \frac{(45)^2(10^{-6}) e_g^2}{f (e_g + 3) 10^{-11}} \frac{1}{20 f (27.5)(10^{-12}) e_g + 4(10^{-3})}. \quad (11)$$

and is plotted in Fig. 8(b).

1.4 GRAPHICAL CIRCUIT ANALYSIS

Linear circuit analysis is useful in analyzing this type of pulse amplifier in an approximate manner. It tells one the tube parameters which are important and gives one the ability to estimate with very little calculation the number of gate drives that may be expected from a particular amplifier configuration. If a more precise description of the pulse waveform is desired, one can resort to a graphical analysis of the pulse amplifier.

1.4.1 General discussion.—If the grid signal waveform is assumed to be known, then from the plate characteristics of the tube and a known RLC load, the output-voltage waveform may be plotted. From the same set of calculations, the magnetizing current, the capacitive current, the load current, and the total tube current and voltage may be plotted. If the tube has a screen grid, and if the screen-grid characteristics are available, then a plot of screen-grid current may also be obtained by reading from the screen current, point by point, for the previously calculated pairs of values of plate voltage and control-grid voltage.

The transformer and its load may be approximated by the circuit of Fig. 9. The leakage inductance is small[3] and may be

3. R. Denton, W. Brown, and W. Kilmer, Computer Components Development, Report No. 2, p. 12, Table I, January 1957.

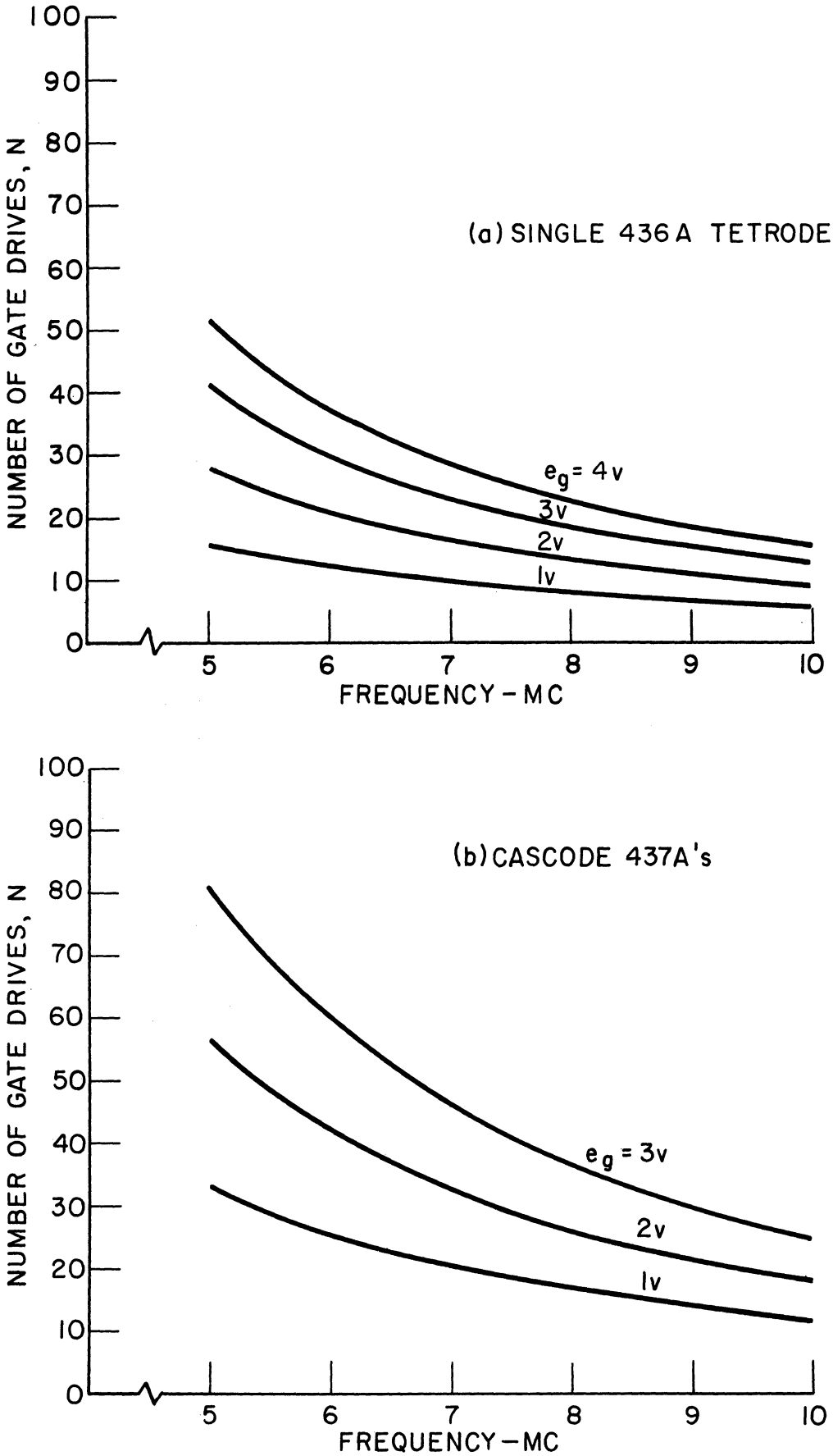

Fig. 8. Variation of number of gate drives with frequency.

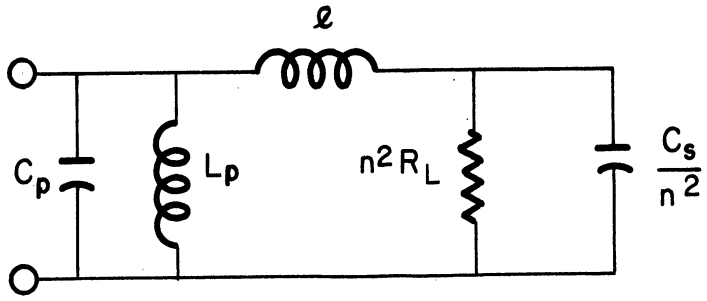

ℓ = Transformer leakage inductance
L_p = Transformer primary inductance
C_p = Primary shunt capacitance
C_s = Secondary shunt capacitance
R_L = Secondary load resistance
n = Step-down turns ratio

Fig. 9. Approximate transformer equivalent circuit.

neglected without serious error. In this case, the plate load for the tube reduces to a parallel RLC circuit as in Fig. 10.

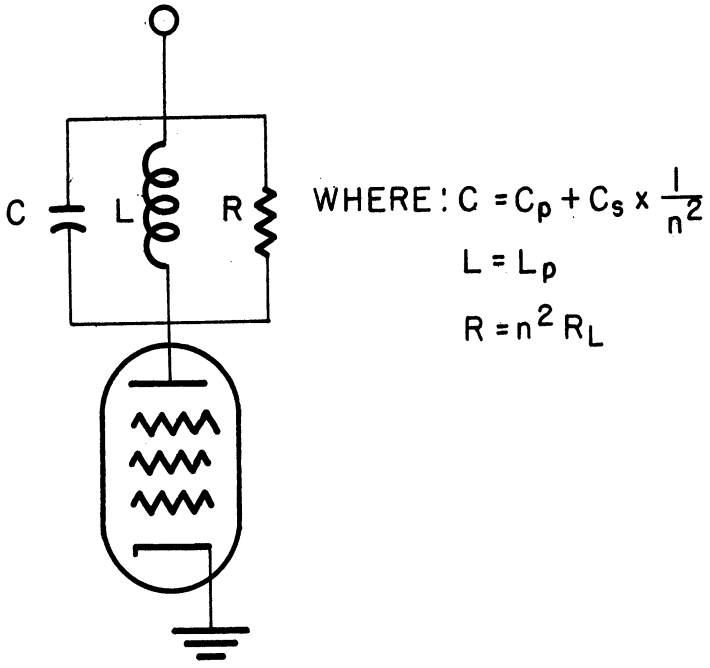

Fig. 10. Approximate plate load presented by the transformer and its load.

The essence of the analysis is that the grid waveform may be approximated by true step functions occurring at regular intervals of time as in Fig. 11. The approximation becomes more accurate as the number of steps is increased and the time between steps is decreased. The approximation becomes exact in the limit as the number of steps tends to infinity and the time between steps tends to zero.

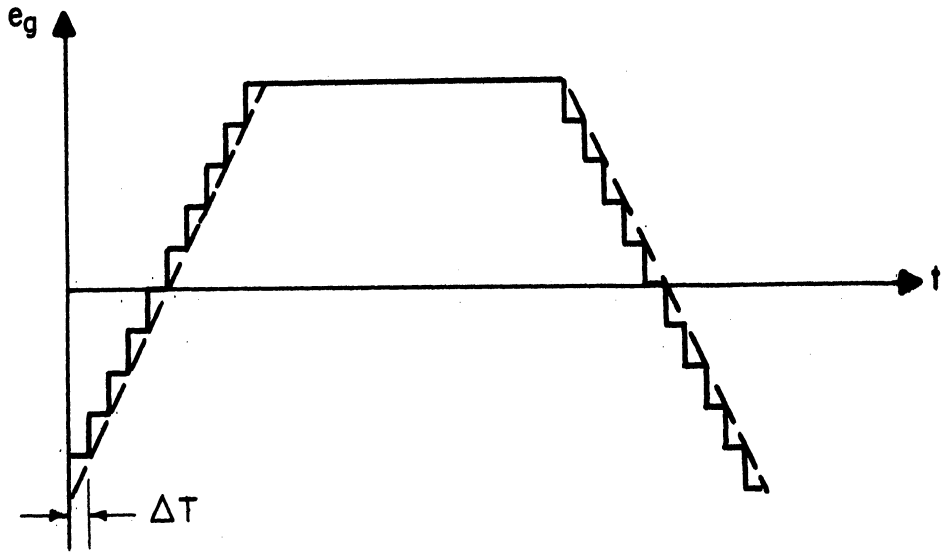

Fig. 11. Approximation of a waveform by steps.

The steps of voltage at the grid will result in steps of current through the tube. The tube current-step increase may flow through any of the three paths: R, L, or C. However, a true step increase will flow through C at the initial instant of application, and, if sufficiently short times, Δt, are used, then it is approximately true that the capacitor current will not change appreciably during one time interval. Hence, the voltage across the capacitor will increase during the first interval, and during the second interval this voltage will begin to force current through the resistive load according to Ohm's Law and will begin to change the current in the inductance according to Lenz's Law. Note that an error has been introduced: actually some resistive current will flow as soon as the capacitor has acquired the most minute charge, and also the inductive current will begin to change. However, if the time interval is taken quite small, then the error will be small.

Before the pulse is applied, the grid is at some steady potential, there is some steady flow of plate current, and all this current flows through the primary of the transformer, which is a d-c short circuit. Hence, initially, there is no output voltage e_p and

there is no current in either the capacitor or the resistor. Then at $t = 0+$, the grid voltage is suddenly increased and causes a sudden increase in the plate current of i_{b_1}. The problem to be solved then is as illustrated in Fig. 12.

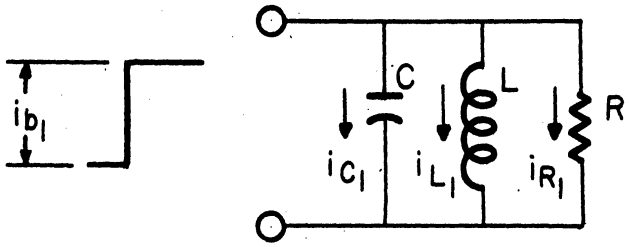

Fig. 12. The problem arising from a step grid voltage.

For times $t \ll RC$, the currents may be shown to be approximately

$$i_{R_1} = i_{b_1} \frac{t}{RC} \left(1 - \frac{t}{2\,RC}\right) \tag{13}$$

$$i_{L_1} = i_{b_1} \left(\frac{t}{2\,RC}\right)^2 \tag{14}$$

$$i_{C_1} = i_{b_1} \left(1 - \frac{t}{2\,RC}\right)^2 , \tag{15}$$

provided that the circuit is critically damped. Presumably the increase in plate current i_{b_1} is not known. However, it is known that the output voltage is given by[1]

$$e_{P_1} = E_{bb} - e_{b_1} , \tag{16}$$

and it is also known that the output voltage must be given by

$$e_{P_1} = \frac{1}{C} \int i_{C_1}\, dt = i_{R_1} R = L \frac{di_{L_1}}{dt} . \tag{17}$$

If we now apply the approximation that the capacitive current is a constant for short times, we have

$$e_{P_1} = i_{C_1} \frac{t}{C} \text{ for } t \ll RC . \tag{18}$$

and at the end of the first interval we have

$$i_{C_1} \frac{\Delta t}{C} = E_{bb} - e_{b_1} , \tag{19}$$

where $t = \Delta t-$ (just before the second grid step), and

e_{b_1} = the plate voltage at $t = \Delta t-$ and is unknown.

But i_{c_1} is given by

$$i_{c_1} = i_{b_1} - i_{R_1} - i_{L_1} . \tag{20}$$

Therefore,

$$\left(i_{b_1} - i_{R_1} - i_{L_1}\right) \frac{\Delta t}{C} = E_{bb} - e_{b_1} . \tag{21}$$

This last equation may be rewritten in the form of a load line, drawn on the plate characteristics, and e_{b_1} and i_{b_1} read off. Given e_{b_1} and i_{b_1}, the currents i_{c_1}, i_{L_1}, and i_{r_1} may be calculated. This procedure may be generalized to the following recursion formulae:

$$E_j = E_{bb} + (i_{r_{j-1}} + i_{L_{j-1}}) \Delta t/C - e_{p_{j-1}} \tag{22}$$

$$e_{b_j} = E_j - (\Delta t/C) i_{b_j} \tag{23}$$

$$e_{p_j} = E_{bb} - e_{b_j} \tag{24}$$

$$i_{r_j} = e_{p_j}/R \tag{25}$$

$$i_{L_j} = i_{L_{j-1}} + e_{p_j}(\Delta t/L) \tag{26}$$

$$i_{c_j} = i_{b_j} - i_{R_j} - i_{L_j} \tag{27}$$

From these equations, known initial conditions, given grid waveform, and the plate characteristics of the tube used, a complete solution may be obtained.

1.4.2 A specific example of graphical analysis.—The discussion of the preceeding section and the method of applying the formulae to a particular situation can probably be clarified by consideration of a particular example.

Consider the cascode 437A circuit of Fig. 13 with input grid signal as in Fig. 14 and plate characteristics as in Fig. 15. Assume a transformer primary inductance of 200 μhy, a shunt capacitance of 10 pF, and a load resistance referred to the primary of 2k (this value of resistance slightly overdamps the circuit). The plate supply voltage will be taken as 200 volts and the upper grid supply as 75 volts.

Assuming that there has been no input pulse for a sufficiently long time for all transients to have died out, all the plate current will flow through the inductance, and there will be no output voltage and no

resistive or capacitive component of current. The grid voltage will be -1.0 volt. Evaluating Eq. (22) for these conditions gives E_o = 203.2 volts and substituting into Eq. (23) gives

$$e_{b_o} = 203.2 - 200\, i_{b_o} \quad . \tag{28}$$

This load line is the j = 0 line of Fig. 15, and at the intersection with the e_g = -1.0-volt curve, one can read e_{b_o} and i_{b_o} to be 200 volts and 16 ma, respectively. From Eq. (24) through (27), respectively, one calculates e_{p_o} = 0, i_{r_o} = 0, i_{L_o} = 16 ma, and i_{c_o} = 0. This concludes the first iteration.

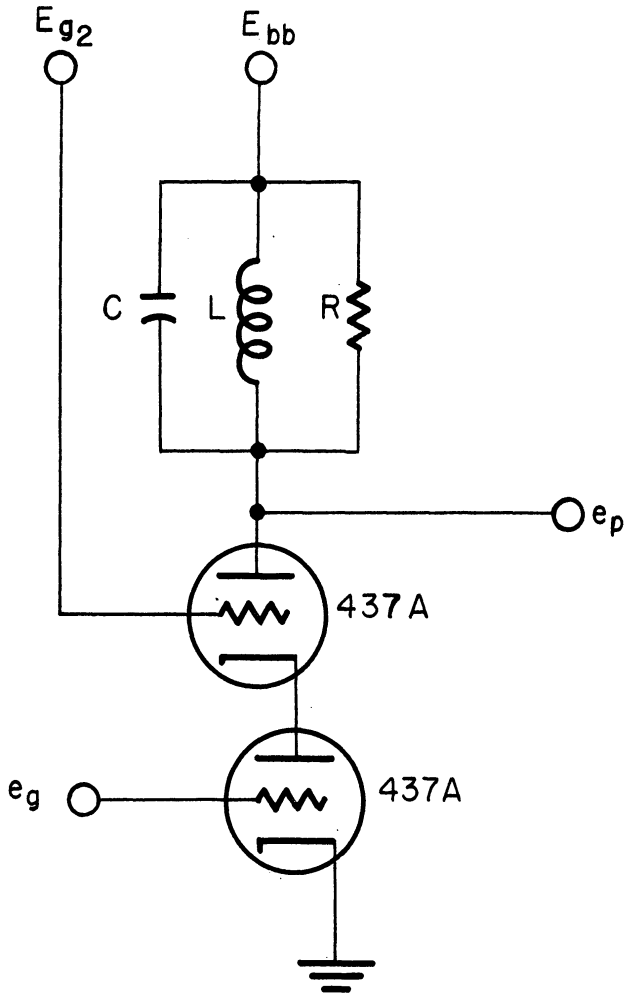

Fig. 13. Cascode circuit used in the graphical analysis example. C = tube interelectrode capacitance, plus stray capacitance = 10 pF; L = 150 μhy; R = 2K.

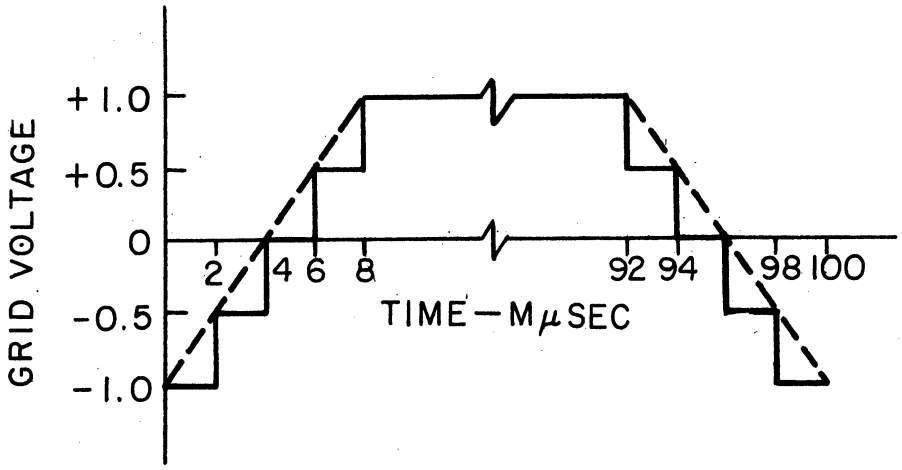

Fig. 14. Input signal.

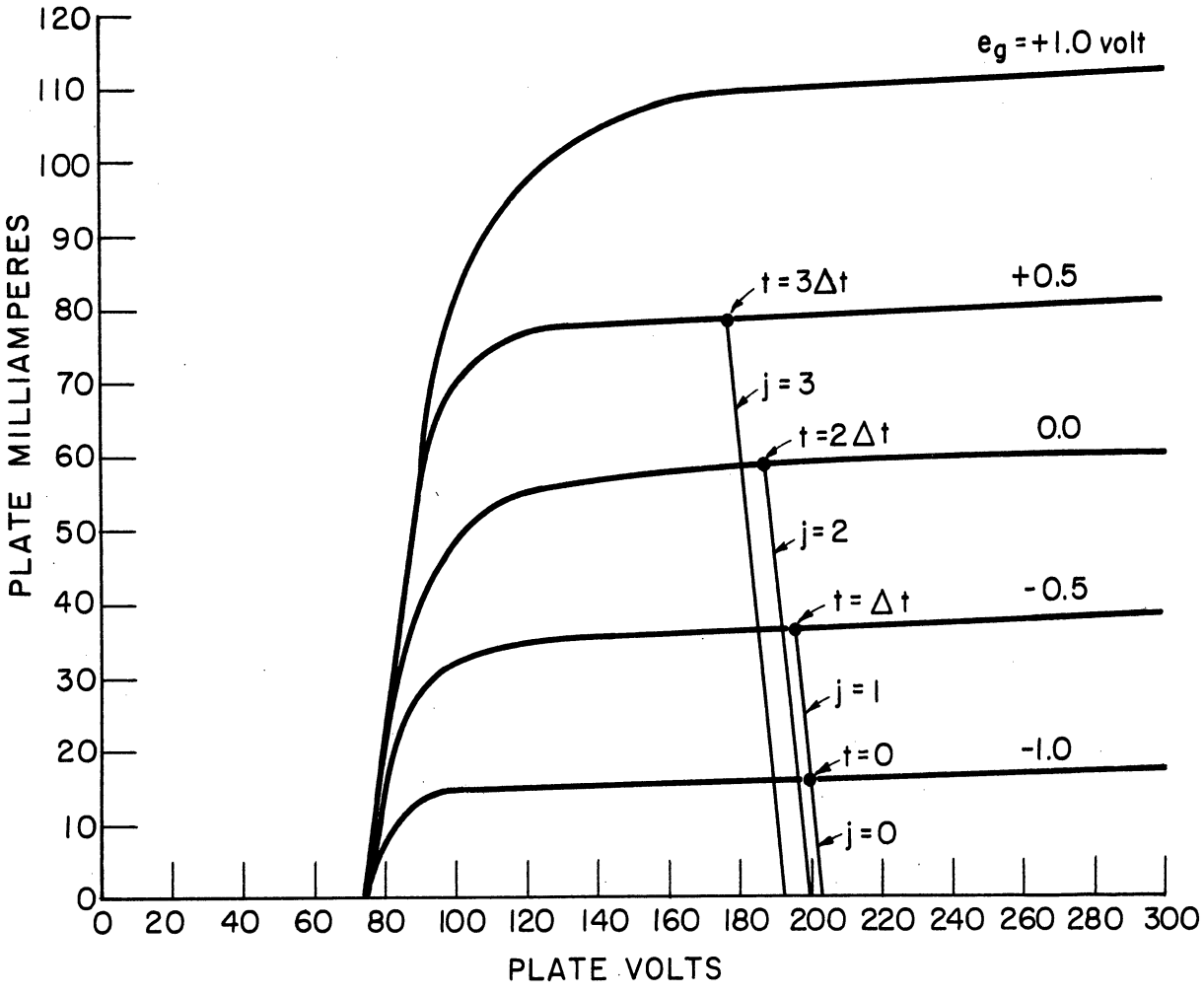

Fig. 15. Plate characteristics for graphical analysis.

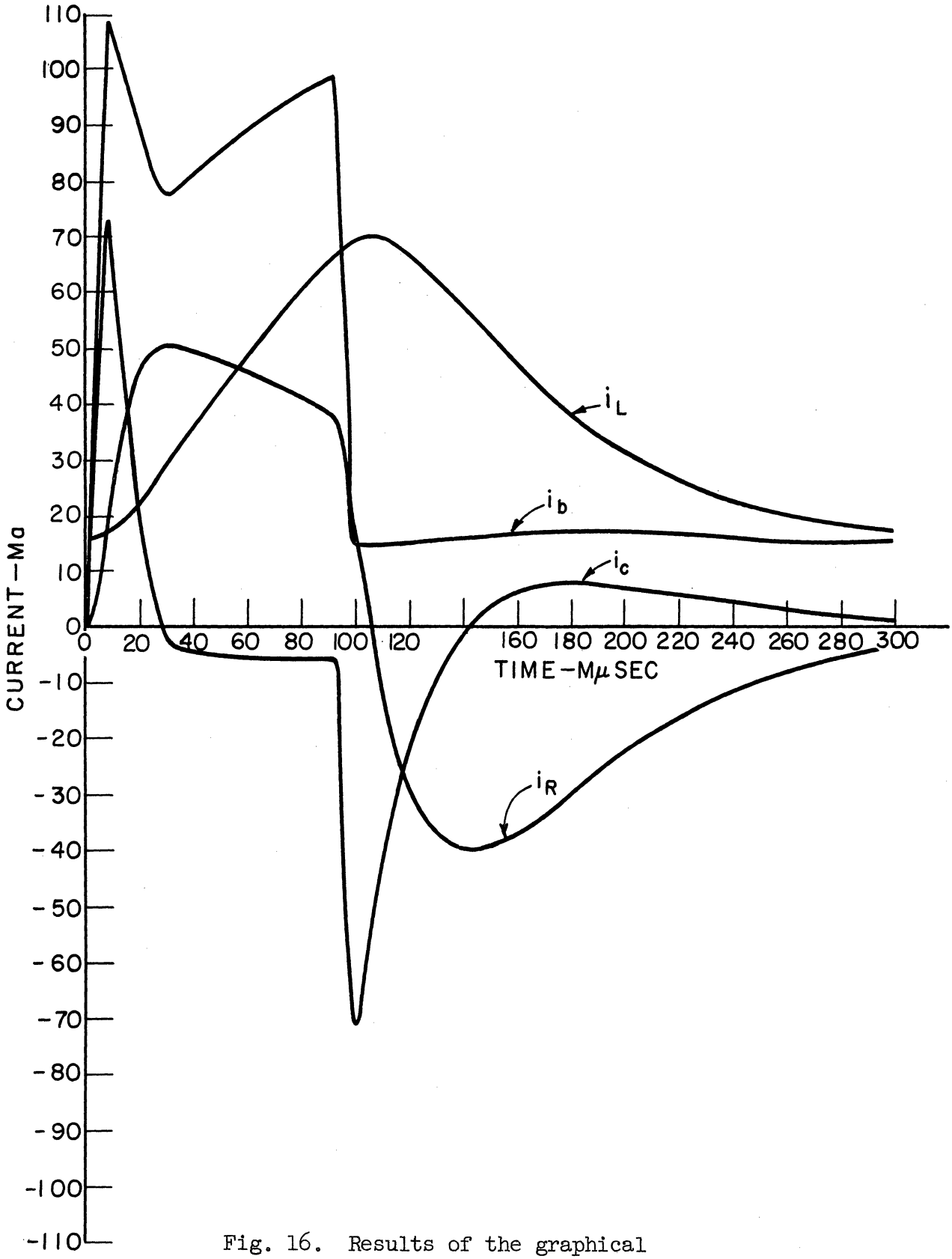

Fig. 16. Results of the graphical analysis example.

For the second iteration, j = 1, t = Δt = 2 mμ sec, and the grid voltage has increased to -0.5 volt, as in Fig. 14. Equation (22) is again evaluated to be

$$E_1 = 203.2 \text{ volts} , \tag{29}$$

Therefore, Eq. (23) is again

$$e_{b_1} = 203.2 - 200\, i_{b_1} . \tag{30}$$

From the intersection of this j = 1 load line with the e_g = 0.5-volt curve, e_{b_1} and i_{b_1} are read as 196 volts and 36 ma, respectively. From Eq. (24) through (27), one calculated, respectively, ep_1 = 4 volts, i_{r_1} = 2 ma, i_{L_1} = 16.05 ma, and i_{c_1} = 18 ma. The second iteration is now ended. Further iterations may be performed similarly with the results being as shown in Table I. These results are presented graphically in Fig. 16. Experimental results using the same voltages and circuit parameters are presented for comparison in the photograph of plate voltage in Fig. 17.

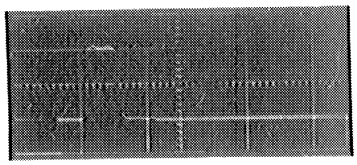

(a) Grid waveform
1 volt/major division
100 mμsec/major division

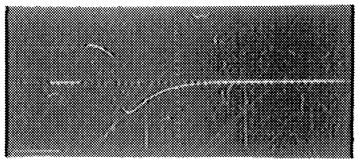

(b) Plate waveform
100 volts/major division
100 mμsec/major division

Fig. 17. Experimental waveforms.

The graphical method of analysis yields results which agree quite well with experimental results. However, it is a very time-consuming method and, therefore, does not lend itself to an investigation of the effects of varying circuit parameters if calculations are performed by hand. Therefore, the problem of programming an automatic computer to perform the graphical analysis routine is presently being considered. Such a program can be modified easily, or even automatically, so that circuit parameters can be varied at will. Furthermore, the speed of a computer as compared with hand computation makes feasible the analysis of a circuit when subjected to a train of pulses rather than just an isolated pulse, as considered here. Any differences between the first and Nth pulses of the train can be observed as can the build-up of the magnetizing current to its steady-state waveform. The load current can be varied to determine the ultimate number of gate drives. Average powers and currents can be computed for each set of impressed voltage and load conditions. Briefly, this

TABLE I

RESULTS OF THE GRAPHICAL ANALYSIS EXAMPLE

j	e_{g_j}	e_{b_j}	i_{b_j}	e_{P_j}	i_{R_j}	i_{L_j}	i_{C_j}	E_j	t
0	-1	200	16	0	0	16.00	0	203.2	0
1	-0.5	196	36	4	2	16.05	18	203.2	2
2	0.0	188	58	12	6	16.21	35.8	199.6	4
3	+0.5	178	79	22	11	16.50	51.5	192.44	6
4	+1.0	162	109	38	19	16.90	73.1	183.5	8
5	+1.0	149	106	51	25.5	17.58	63	169.2	10
6	+1.0	138	104	62	31	18.4	54.6	157.6	12
7	+1.0	128	100	72	36	19.36	44.6	147.7	14
8	+1.0	120	97	80	40	20.42	36	139	16
9	+1.0	114	93	86	43	21.56	29.4	132.1	18
10	+1.0	108	90	92	46	22.8	21.2	126.9	20
11	+1.0	105	86	95	47.5	24.06	14.4	121.8	22
12	+1.0	102	83	98	49	25.36	8.6	119.3	24
13	+1.0	100	80	100	50	26.69	3.3	116.9	26
14	+1.0	99.5	79	100.5	50.25	28.03	0.72	115.3	28
15	+1.0	98.6	77.5	101.4	50.7	29.38	- 2.58	114.2	30
16	+1.0	99	78	101	50.5	30.72	- 3.22	114.6	32
17	+1.0	99.5	79	100.5	50.25	32.06	- 3.31	115.24	34
18	+1.0	100	80	100	50	33.39	- 3.39	116	36
19	+1.0	100.6	80.7	99.4	49.7	34.71	- 3.7	116.7	38
20	+1.0	101.1	81.2	98.9	49.5	36.03	- 4.33	117.5	40
21	+1.0	101.8	82.1	98.2	49.1	37.34	- 4.34	118.2	42
22	+1.0	102.4	83	97.6	48.8	38.64	- 4.44	119.1	44
23	+1.0	103	84	97	48.5	39.94	- 4.44	119.9	46
24	+1.0	103.8	84.7	96.2	48.1	41.32	- 4.72	120.67	48
25	+1.0	104.5	85.3	95.5	47.8	42.59	- 5.09	121.7	50
26	+1.0	105.3	86.1	94.7	47.35	43.85	- 5.1	122.6	52
27	+1.0	106	87	94	47	45.10	- 5.1	123.54	54
28	+1.0	106.8	87.9	93.2	46.6	46.34	- 5.04	124.42	56
29	+1.0	107.7	88.6	92.3	46.15	47.57	- 5.12	125.4	58
30	+1.0	108.4	89.2	91.6	45.8	48.79	- 5.39	126.4	60
31	+1.0	109.1	90	90.9	45.45	50.00	- 5.45	127.32	62
32	+1.0	110	90.4	90	45	51.20	- 5.80	128.2	64
33	+1.0	111	91.2	89	44.5	52.38	- 5.68	129.24	66
34	+1.0	112	92	88	44	53.55	- 5.55	130.38	68

TABLE I (Continued)

j	e_{g_j}	e_{b_j}	i_{b_j}	e_{P_j}	i_{R_j}	i_{L_j}	i_{C_j}	E_j	t
35	+1.0	112.9	92.9	87.1	43.55	54.71	- 5.36	131.51	70
36	+1.0	113.8	93.4	86.2	43.1	55.86	- 5.56	132.55	72
37	+1.0	114.6	94	85.4	42.7	57.00	- 5.70	133.59	74
38	+1.0	115.7	94.7	84.3	42.15	58.12	- 5.57	134.54	76
39	+1.0	116.7	95.1	83.3	41.65	59.23	- 5.78	135.8	78
40	+1.0	117.7	95.9	82.3	41.15	60.31	- 5.56	136.9	80
41	+1.0	118.5	96.3	81.5	40.75	61.40	- 5.85	138.0	82
42	+1.0	119.7	97	80.3	40.15	62.47	- 5.62	138.9	84
43	+1.0	120.6	97.6	79.4	39.7	63.53	- 5.63	140.2	86
44	+1.0	121.6	98	78.4	39.2	64.57	- 5.77	141.25	88
45	+1.0	122.7	98.6	77.3	38.65	65.60	- 5.65	142.35	90
46	+1.0	123.7	99	76.3	38.15	66.61	- 5.76	143.35	92
47	+0.5	129.1	77	70.9	35.45	67.55	-26	144.65	94
48	0.0	138.3	56	61.7	30.85	68.37	-43.22	149.7	96
49	-0.5	151	35	49	24.5	69.02	-58.52	158.14	98
50	-1.0	166.6	15.1	33.4	16.7	69.46	-71.06	169.7	100
51	-1.0	179.8	15.1	20.2	10.1	70.33	-65.33	182.83	102
52	-1.0	192.7	15.4	7.3	3.65	70.43	-58.68	195.9	104
53	-1.0	204.4	15.7	- 4.4	- 2.2	70.37	-52.47	207.5	106
54	-1.0	214.0	15.9	-14.0	- 7.0	70.28	-47.38	217.0	108
55	-1.0	223.5	16.0	-23.5	-11.75	69.96	-42.21	226.7	110
56	-1.0	231.8	16.0	-31.8	-15.9	69.54	-37.64	235.1	112
57	-1.0	239.3	16.0	-39.3	-19.65	69.02	-33.37	242.5	114
58	-1.0	246	16.0	-46	-23	68.41	-29.41	249.2	116
59	-1.0	252	16.1	-52	-26	67.72	-25.72	255.1	118
60	-1.0	257	16.2	-57	-28.5	66.96	-22.26	260.3	120
61	-1.0	261.3	16.2	-61.3	-30.65	66.14	-19.29	264.7	122
62	-1.0	265.1	16.3	-65.1	-32.55	65.27	-16.42	268.4	124
63	-1.0	268.1	16.3	-68.1	-34.05	64.36	-14.01	271.6	126
64	-1.0	270.9	16.4	-70.9	-35.45	63.42	-11.57	274.2	128
65	-1.0	272.1	16.5	-72.1	-36.05	62.46	- 9.91	275.5	130
66	-1.0	274.0	16.6	-74	-37	61.48	- 7.88	277.3	132
67	-1.0	275.7	16.6	-75.7	-37.85	60.47	- 6.02	278.9	134
68	-1.0	276.9	16.6	-76.9	-38.45	59.45	- 4.4	280.2	136
69	-1.0	277.9	16.7	-77.9	-38.95	58.44	- 2.79	281.1	138
70	-1.0	278.7	16.7	-78.7	-39.35	57.39	- 1.34	281.9	140
71	-1.0	279.0	16.7	-79.0	-39.5	56.34	- 0.14	282.3	142
72	-1.0	279.1	16.7	-79.1	-39.55	55.29	+ 0.96	282.4	144
73	-1.0	278.8	16.7	-78.8	-39.4	54.24	+ 1.86	282.1	146

TABLE I (Continued)

j	e_{g_j}	e_{b_j}	i_{b_j}	e_{P_j}	i_{R_j}	i_{L_j}	i_{C_j}	E_j	t
74	-1.0	278.5	16.7	-78.5	-39.25	53.20	+ 2.75	281.8	148
75	-1.0	278.0	16.7	-78.0	-39	52.16	+ 3.54	281.3	150
76	-1.0	277.3	16.7	-77.3	-38.65	51.13	+ 4.22	280.6	152
77	-1.0	276.5	16.6	-76.5	-38.25	50.11	4.74	279.8	154
78	-1.0	275.7	16.6	-75.7	-37.85	49.10	5.35	278.9	156
79	-1.0	274.8	16.6	-74.8	-37.4	48.11	5.89	277.95	158
80	-1.0	273.7	16.6	-73.7	-36.85	47.13	6.32	276.94	160
81	-1.0	272.5	16.5	-72.5	-36.25	46.17	6.58	275.8	162
82	-1.0	271.2	16.5	-71.2	-35.6	45.22	6.88	274.5	164
83	-1.0	270.0	16.5	-70.0	-35	44.28	7.22	273.1	166
84	-1.0	268.6	16.4	-68.6	-34.3	43.37	7.33	271.9	168
85	-1.0	267.2	16.3	-67.2	-33.6	42.48	7.42	270.4	170
86	-1.0	265.9	16.3	-65.9	-32.95	41.61	7.64	269	172
87	-1.0	264.3	16.3	-64.3	-32.15	40.75	7.70	267.6	174
88	-1.0	262.8	16.2	-62.8	-31.4	39.94	7.66	266	176
89	-1.0	261.1	16.2	-61.1	-30.55	39.13	7.62	264.5	178
90	-1.0	259.7	16.2	-59.7	-29.85	38.34	7.71	262.8	180
91	-1.0	258.0	16.2	-58.0	-29.0	37.57	7.63	261.4	182
92	-1.0	256.4	16.1	-56.4	-28.2	36.82	7.48	259.7	184
93	-1.0	255	16.1	-55	-27.5	36.09	7.51	258.1	186
94	-1.0	253.4	16.1	-53.4	-26.7	35.38	7.42	256.7	188
95	-1.0	252	16.1	-52	-26.0	34.69	7.41	255.1	190
96	-1.0	250.4	16.0	-50.4	-25.2	34.02	7.18	253.7	192
97	-1.0	249.0	16.0	-49	-24.5	33.37	7.13	252.2	194
98	-1.0	247.6	16.0	-47.6	-23.8	32.74	7.06	250.8	196
99	-1.0	246	16.0	-46	-23	32.13	6.87	249.4	198
100	-1.0	244.4	16.0	-44.4	-22.2	31.54	6.66	247.8	200
101	-1.0	243	16.0	-43	-21.5	30.97	6.53	246.3	202
102	-1.0	241.7	16.0	-41.7	-20.85	30.42	6.43	244.9	204
103	-1.0	240.4	16.0	-40.4	-20.2	29.88	6.22	243.6	206
104	-1.0	239.2	16.0	-39.2	-19.6	29.36	6.24	242.4	208
105	-1.0	238.0	16.0	-38	-19	28.86	6.14	241.2	210
106	-1.0	236.9	16.0	-36.9	-18.45	28.37	6.08	240.0	212
107	-1.0	235.9	16.0	-35.9	-17.95	27.90	6.05	238.9	214
108	-1.0	234.8	16.0	-34.8	-17.4	27.44	5.96	237.9	216
109	-1.0	233.8	16.0	-33.8	-16.9	26.99	5.91	236.8	218
110	-1.0	232.6	16.0	-32.6	-16.3	26.56	5.74	235.8	220
111	-1.0	231.4	16.0	-31.4	-15.7	26.14	5.56	234.6	222
112	-1.0	230.3	16.0	-30.3	-15.15	25.74	5.41	233.4	224

TABLE I (Concluded)

j	e_{g_j}	e_{b_j}	i_{b_j}	e_{P_j}	i_{R_j}	i_{L_j}	i_{C_j}	E_j	t
113	-1.0	229.5	16.0	-29.5	-14.75	25.35	5.40	232.4	226
114	-1.0	228.4	16.0	-28.4	-14.2	24.98	5.22	231.6	228
115	-1.0	227.4	16.0	-27.4	-13.7	24.62	5.08	230.6	230
116	-1.0	226.4	16.0	-26.4	-13.2	24.27	4.93	229.6	232
117	-1.0	225.3	16.0	-25.3	-12.65	23.94	4.71	228.6	234
118	-1.0	224.4	16.0	-24.4	-12.2	23.62	4.18	227.5	236
119	-1.0	223.9	16.0	-23.9	-11.95	23.30	4.65	226.8	238
120	-1.0	223.0	16.0	-23	-11.5	23.00	4.50	226.2	240
121	-1.0	222.1	16.0	-22.1	-11.05	22.71	4.34	225.3	242
122	-1.0	221.3	15.9	-21.3	-10.65	22.43	4.12	224.4	244
123	-1.0	220.5	15.9	-20.5	-10.25	22.16	3.99	223.7	246
124	-1.0	219.8	15.9	-19.8	- 9.9	21.90	4.0	222.9	248
125	-1.0	218.9	15.9	-18.9	- 9.45	21.66	3.69	222.2	250
126	-1.0	218.1	15.9	-18.1	- 9.05	21.42	3.53	221.3	252
127	-1.0	217.5	15.9	-17.5	- 8.75	21.19	3.46	220.6	254
128	-1.0	216.9	15.9	-16.9	- 8.45	20.97	3.38	220.0	256
129	-1.0	216.4	15.8	-16.4	- 8.2	20.75	3.35	219.4	258
130	-1.0	215.7	15.8	-15.7	- 7.85	20.54	3.11	218.9	260
131	-1.0	215.0	15.8	-15.0	- 7.50	20.34	2.96	218.2	262
132	-1.0	214.3	15.8	-14.3	- 7.15	20.15	2.80	217.6	264
133	-1.0	213.8	15.7	-13.8	- 6.9	19.97	2.73	216.9	266
134	-1.0	213.3	15.7	-13.3	- 6.65	19.79	2.56	216.4	268
135	-1.0	212.7	15.7	-12.7	- 6.35	19.62	2.43	215.9	270
136	-1.0	212.3	15.7	-12.3	- 6.15	19.46	2.39	215.4	272
137	-1.0	212.0	15.7	-12.0	- 6.0	19.30	2.40	215.0	274
138	-1.0	211.4	15.7	-11.4	- 5.7	19.15	2.25	214.6	276
139	-1.0	211.0	15.7	-11.0	- 5.5	19.01	2.19	214.1	278
140	-1.0	210.5	15.7	-10.5	- 5.25	18.87	2.08	213.7	280
141	-1.0	210.0	15.7	-10.0	- 5.0	18.74	1.96	213.2	282
142	-1.0	209.5	15.7	- 9.5	- 4.75	18.61	1.84	212.7	284
143	-1.0	209.1	15.7	- 9.1	- 4.55	18.49	1.86	212.3	286
144	-1.0	208.7	15.7	- 8.7	- 4.35	18.37	1.72	211.9	288
145	-1.0	208.3	15.7	- 8.3	- 4.15	18.26	1.59	211.5	290
146	-1.0	207.9	15.7	- 7.9	- 3.95	18.15	1.50	211.1	292
147	-1.0	207.5	15.7	- 7.5	- 3.75	18.05	1.40	210.7	294
148	-1.0	207.2	15.7	- 7.3	- 3.60	17.95	1.35	210.4	296
149	-1.0	207.0	15.7	- 7.0	- 3.50	17.86	1.34	210.2	298
150	-1.0	206.7	15.7	- 6.7	- 3.35	17.77	1.28	209.9	300

analysis can be used to investigate pulse amplifiers in considerable detail and with an accuracy which is consistent with the accuracy of an average family of plate-characteristic curves.

2. EXPERIMENTAL RESULTS AND CIRCUITS

As a check on the validity of our results, an experimental investigation was made of the circuits which had been analyzed theoretically. Since no generator was available which was capable of producing the desired signal input, it was decided that the pulse amplifier should be made to furnish its own input by means of the dynamic flip-flop circuit. Consequently, dynamic flip-flops using the 436A tetrode and cascode 437A triodes have been built and tested. Both of these circuits were designed for 5 mcps operation; the transformers used were chosen to have a primary inductance which allowed for a sufficiently rapid recovery and with a turns ratio which gave the secondary voltage which was necessary to drive the delay lines. Diagrams for the 437A and the 436A circuits are shown in Figs. 18 and 20, respectively.

2.1 437A CASCODE CIRCUIT

This circuit was capable of supplying 200-ma load current before the flip-flop stopped working. The plate and upper-grid supply voltages are the maximum that may be used to remain within the rated 45-ma average cathode current of the tube. Table II gives the plate, upper-grid, and total cathode currents as a function of the load current. The transformer secondary should always be heavily loaded to keep the grid dissipation and cathode current low. Western Electric recommends that the grid dissipation be kept below 20 milliwatts, and this is done in this circuit at all loads. However, the average cathode-current rating is exceeded unless the secondary is loaded.

TABLE II

VARIATION OF TUBE CURRENTS WITH LOAD CURRENT FOR CASCODE 437A'S

I_L (ma)	0	25	50	75	100	125	150
I_P (ma)	24	26	29	31	33	35	36
I_{grid} (ma)	30	26	24	20	17	14	11
$I_{cathode}$ (ma)	54	52	53	51	50	49	47

The 200-ma load current represents about sixteen 12-ma gates that this circuit is capable of driving.

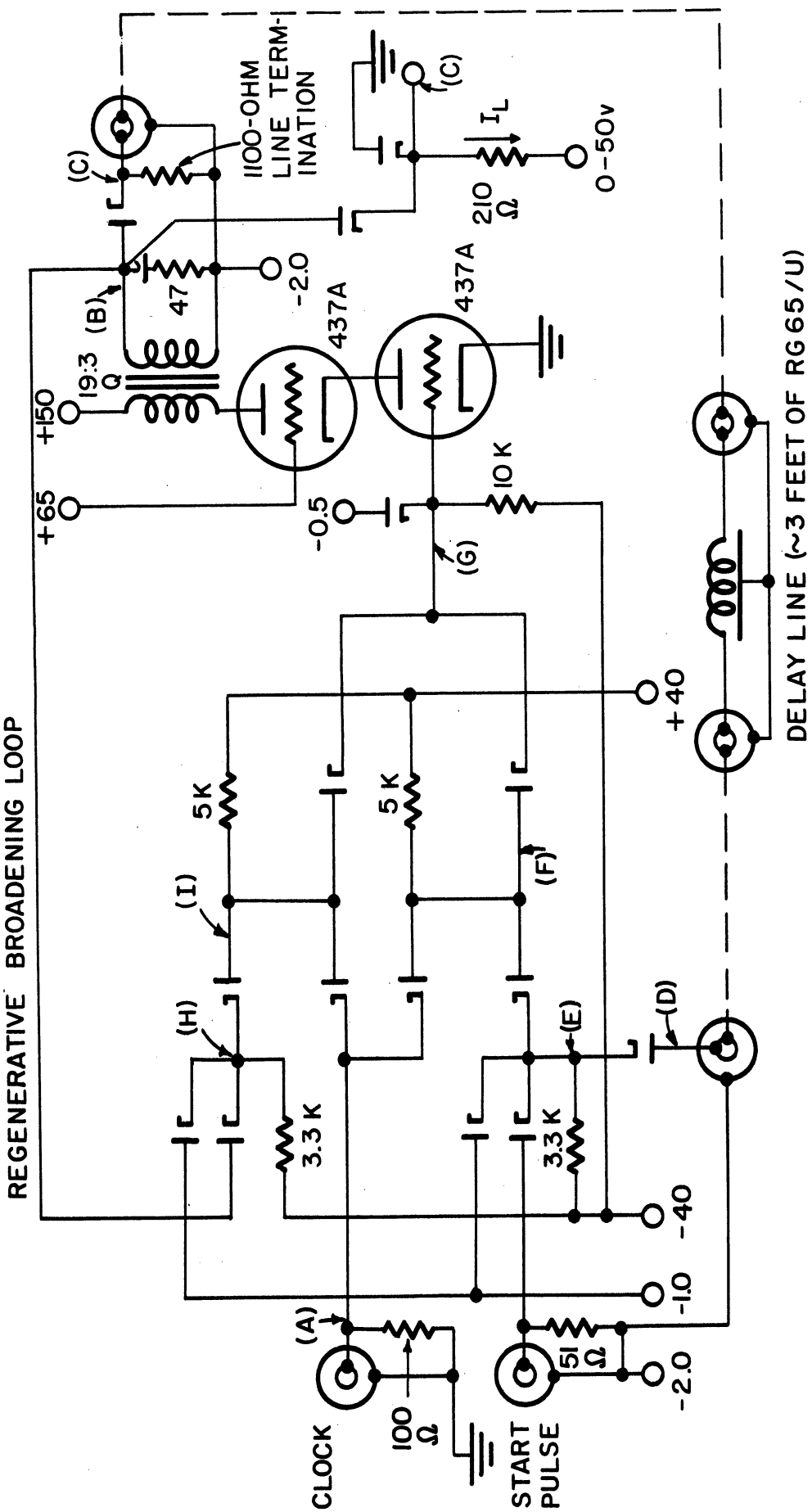

Fig. 18. Cascode 437A dynamic flip-flop for 5-mc operation.

Typical waveforms for this circuit are shown in Fig. 19.

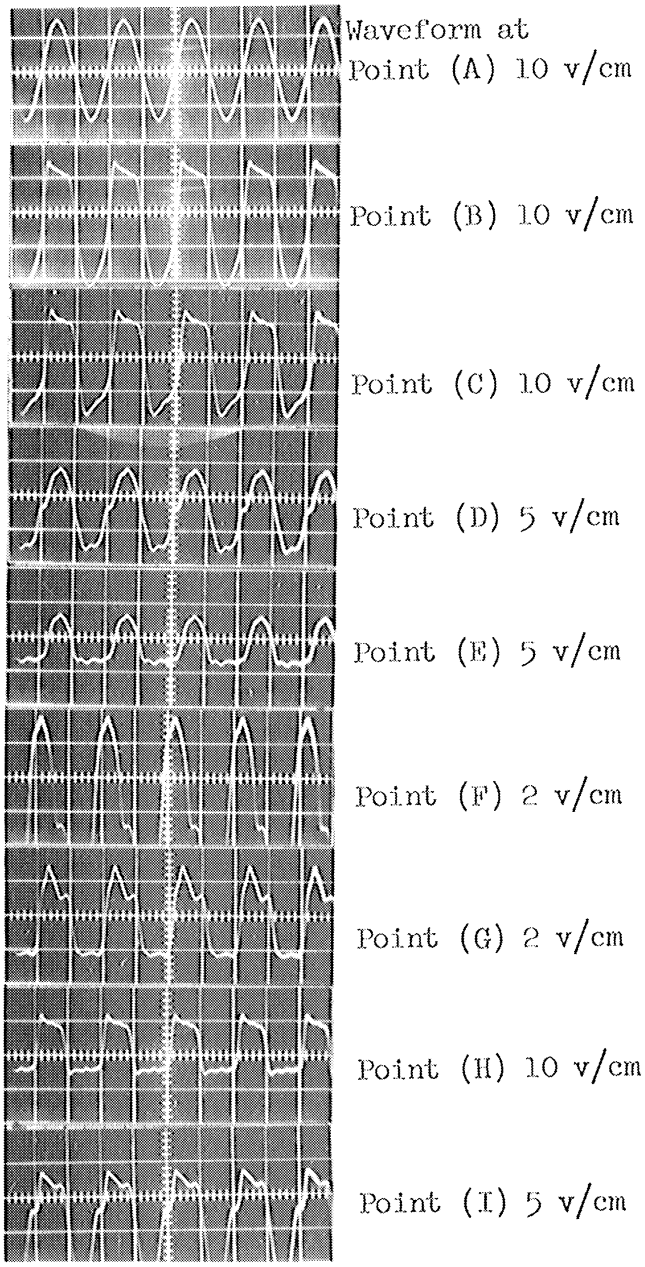

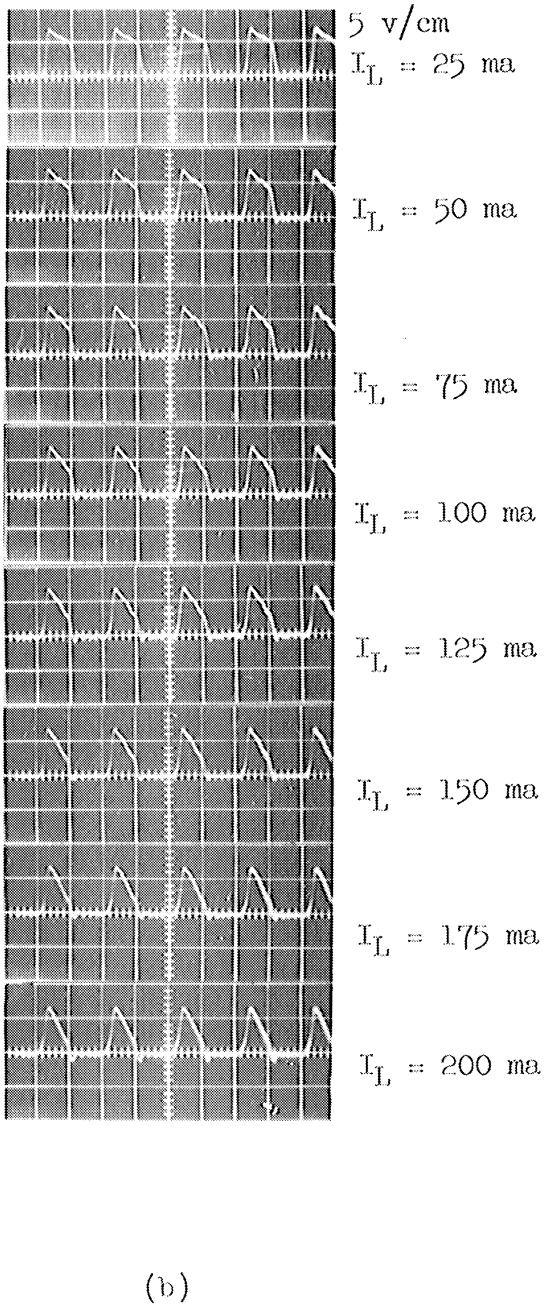

Fig. 19. Waveforms for the 437A flip-flop. (a) Waveforms at various points in the circuit of Fig. 18 for I_L = 25 ma. (b) Waveforms at (c) for the indicated magnitudes of I_L.

2.2 436A CIRCUIT

This circuit becomes inoperative when the load current exceeds

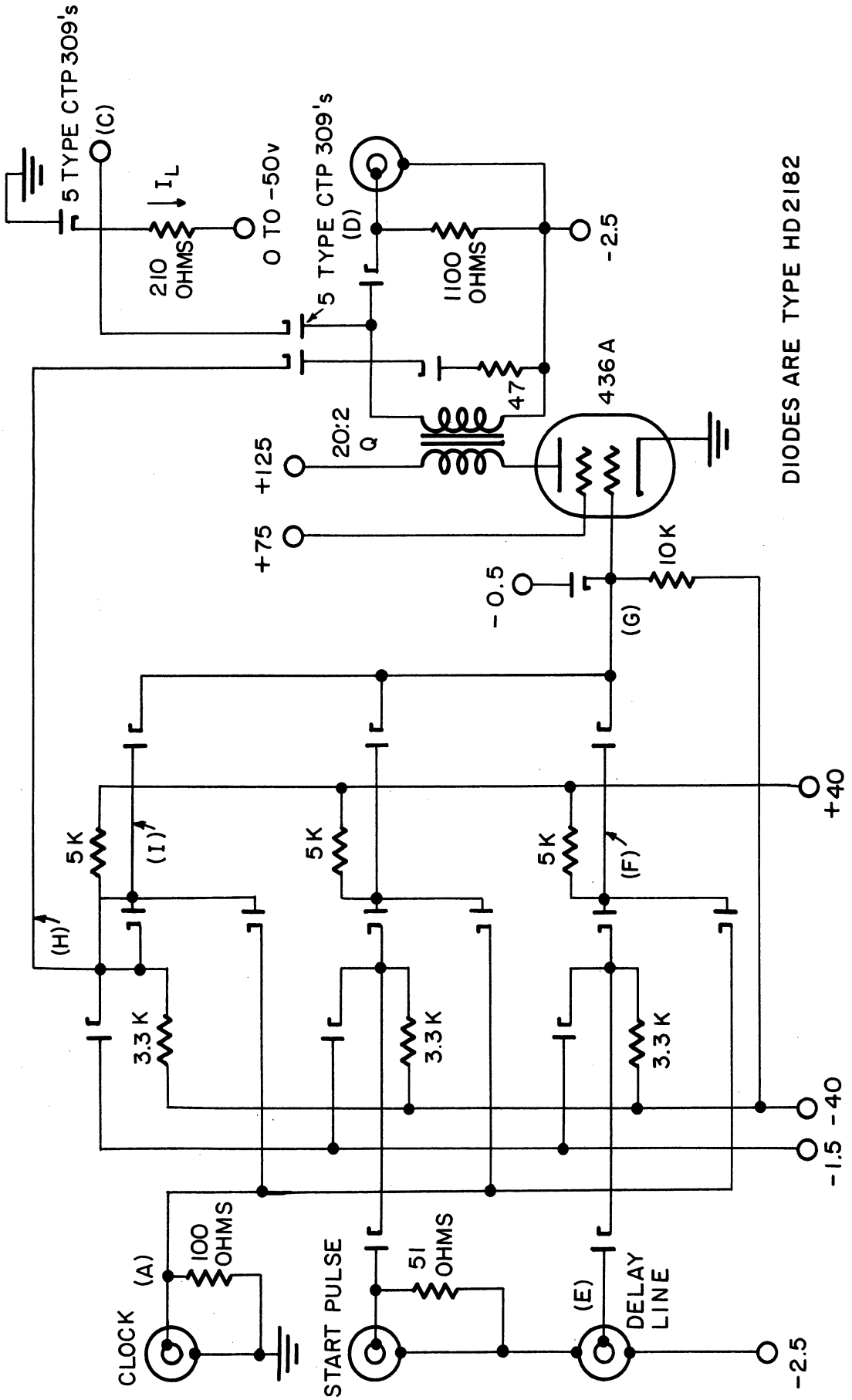

Fig. 20. 436A dynamic flip-flop for 5-mc operation.

350-ma or about twenty-nine 12-ma gates.

Again the transformer secondary should always be loaded in order to keep the screen dissipation below the rated value as indicated in Table III.

Waveforms for this circuit are given in Fig. 21.

TABLE III

VARIATION OF TUBE CURRENTS WITH LOAD CURRENT FOR THE 436A

I_L (ma)	0	25	50	75	100	125	150	175	200
I_P (ma)	15	17	18	19	20	21	22	23	24
I_s (ma)	37	35	34	32	31	30	29	28	26
P_s (watts)	2.77	2.62	2.55	2.4	2.32	2.25	2.17	2.10	1.95

3. CONCLUSIONS

Either the 436A or the cascode 437A circuits work fairly well at 5 mcps and provide enough gate drives to be useful computer packages. Neither of these tubes was able to produce as many gate drives as the theory predicted. This is partially because the gate drives were predicted from a linear circuit analysis, and this type of analysis cannot hope to accurately predict the behavior of this non linear pulse amplifier but can only give more or less qualitative information about the desirable properties of the components to be used. However, the main reason why these circuits are not actually able to produce the number of gate drives predicted is that they are both limited by power or current considerations before the theoretical number of gate drives can be reached. Thus, a more realistic analysis should include the tube limitations on cathode current and power dissipation. The theoretical number of gate drives minus the experimental number indicates roughly the increase in gate drives that we would obtain if the tube dissipation could be increased with the other tube parameters held constant.

Further testing of these 5-mcps circuits will be conducted with a view to determining how they may be interconnected. If it turns out that the interconnection problem can be solved satisfactorily at 5 mcps, then the frequency will be pushed somewhat higher. Preliminary tests with essentially the same circuits, but with different lengths of delay line and with different (lower inductance) transformers, indicate

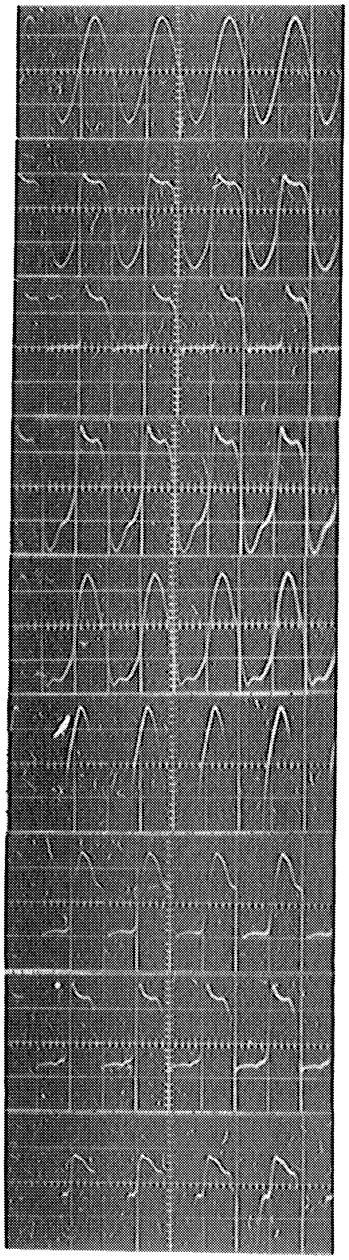

Waveform at
Point (A) 10 v/cm

Point (B) 10 v/cm

Point (C) 5 v/cm

Point (D) 5 v/cm

Point (E) 2 v/cm

Point (F) 2 v/cm

Point (G) 2 v/cm

Point (H) 5 v/cm

Point (I) 5 v/cm

(a)

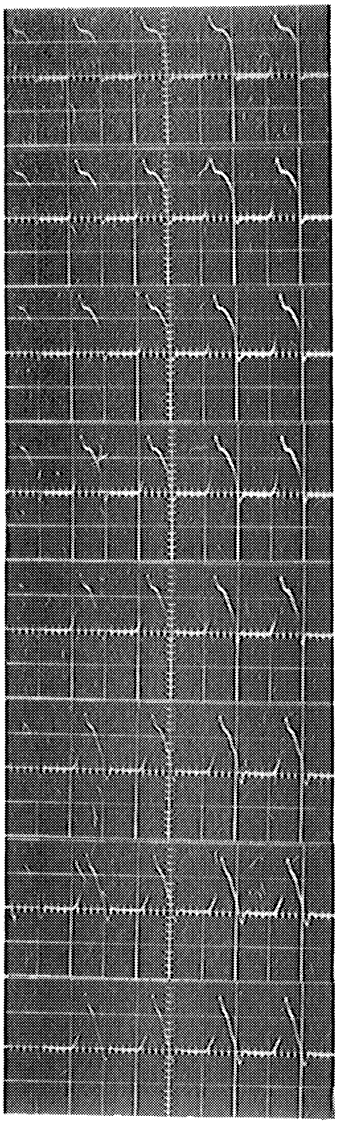

5 v/cm
I_L = 25 ma

I_L = 50 ma

I_L = 75 ma

I_L = 100 ma

I_L = 125 ma

I_L = 150 ma

I_L = 175 ma

I_L = 200 ma

(b)

Fig. 21. Waveforms for 436A flip-flop. (a) Waveforms at various points in the circuit of Fig. 19 for I_L = 25 ma. (b) Waveforms at (c) for the indicated magnitudes of I_L.

that, if the interconnection problem is not too severe, it should be possible to obtain approximately 10 gate drives from the 436A circuit at 7 mcps.

In view of the fact that these pulse amplifiers are limited by current or power ratings, tubes with high power ratings are desirable.

If tubes were available which would deliver a larger plate-current swing than the tubes used here with the same grid-voltage swing, that is, with higher g_m's, then it seems possible to design an amplifier of this type to operate at higher frequencies. However, considering the careful manufacturing processes that were necessary to produce the tubes used here[3], it seems unlikely that significantly better tubes will be developed in the near future[4].

3. Ford, G.T., "The 404A—A Broadband Amplifier Tube," Bell Labs Record, 27, p.59, 1949.

4. Beck, A.H.W., "Thermionic Valves—Their Theory and Design," Cambridge University Press, 1953, p.291.

APPENDIX

TRIODE INPUT CAPACITANCE

The grid is driven by a gating structure which may be approximated by a constant-current step source. The circuit to be considered is then as shown in Fig. 1-A, and the small-signal equivalent of this circuit is shown in Fig. 2-A. Applying Norton's theorem to the voltage generator and letting $R = (r_p R_L)/(r_p + R_L)$ gives the final circuit of Fig. 3-A.

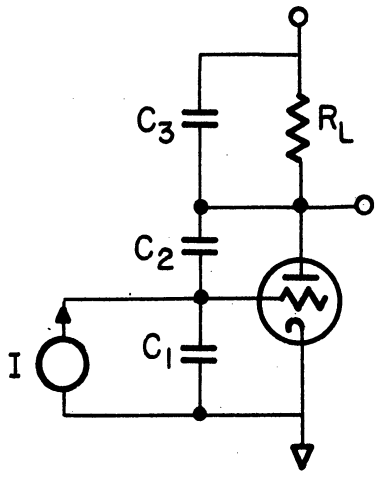

Fig. 1-A

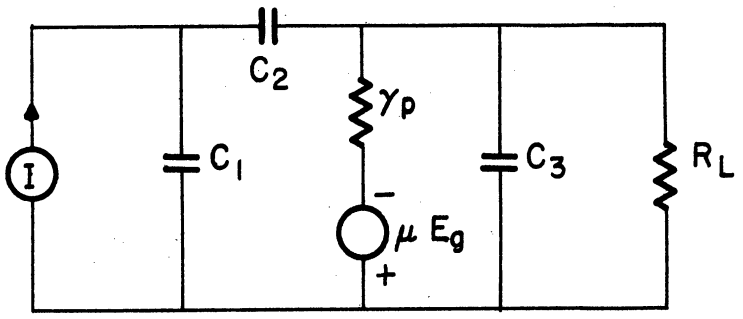

Fig. 2-A

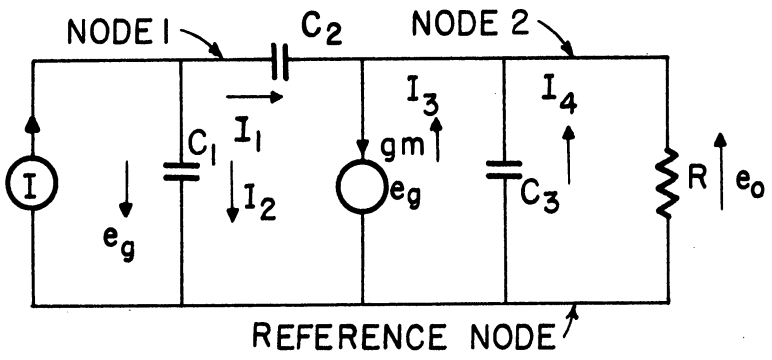

Fig. 3-A

From this last circuit, one may write by inspection

$$I_1 = (e_o + e_g)\, pC_2$$

$$I_2 = e_g\, pC_1$$

$$I_3 = e_o pC_3$$

$$I_4 = \frac{e_o}{R} \quad .$$

For Node 1 $\quad I = I_1 + I_2 = (e_o + e_g)\, pC_2 + e_g\, pC_1$.

For Node 2 $\quad g_m e_g = I_1 + I_3 + I_4 = (e_o + e_g)\, pC_2 + e_o pC_3 + \frac{e_o}{R}$.

Rewriting: $\quad p\,(C_1 + C_2)\, e_g + pC_2 e_o = I$

$$(g_m - pC_2)\, e_g - (pC_2 + pC_3 + \frac{1}{R})\, e_o = 0$$

or:
$$\begin{bmatrix} p(C_1 + C_2) & pC_2 \\ g_m - pC_2 & -p(C_1 + C_3) - \frac{1}{R} \end{bmatrix} \times \begin{bmatrix} e_g \\ e_o \end{bmatrix} = \begin{bmatrix} I \\ o \end{bmatrix}$$

We wish to know the input capacitance, and since

$$e_g = \frac{1}{C_{in}} \int I\, dt \quad \text{or} \quad \frac{de_g}{dt} = \frac{I(t)}{C_{in}} \ ,$$

We then wish to find $(de_g/dt)(1/I(t))$. Hence, solve for pe_g for a step-function input I/p:

$$\frac{pe_g}{I} = \frac{p\,(C_2 + C_3) + \frac{1}{R}}{p\left\{(C_1 + C_2)\left[p(C_2 + C_3) + \frac{1}{R}\right] + C_2(g_m - pC_2)\right\}}$$

$$= \frac{\frac{1 + pR\,(C_2 + C_3)}{R(C_1C_2 + C_1C_3 + C_2C_3)}}{p\left[p + \frac{C_1 + (1 + g_mR)\,C_2}{R(C_1C_2 + C_2C_3 + C_1C_3)}\right]}$$

Let $A = \frac{C_2 + C_3}{C_1C_2 + C_1C_3 + C_2C_3}$,

$B = \frac{1}{R(C_1C_2 + C_1C_3 + C_2C_3)}$, and $\alpha = \frac{C_1 + (1 + g_mR)\,C_2}{R(C_1C_2 + C_1C_3 + C_2C_3)}$.

Then $\frac{pe_g}{I} = \frac{A}{p+\alpha} + \frac{B}{p(p+\alpha)}$,

and $\frac{1}{I}\frac{de_g}{dt} = Ae^{-\alpha t} + \frac{B}{\alpha}(1 - e^{-\alpha t})$

$$= \frac{(C_2 + C_3)\,e^{-\alpha t}}{C_1C_2 + C_1C_3 + C_2C_3} + \frac{(1 - e^{-\alpha t})}{C_1 + (1 + g_mR)\,C_2}$$

$$= \frac{1}{C_1 + (1 + g_mR)\,C_2} + \left[\frac{C_2 + C_3}{C_1C_2 + C_1C_3 + C_2C_3} - \frac{1}{C_1 + (1+g_mR)\,C_2}\right]e^{-\alpha t}$$

$$= \frac{1}{C_{in}} .$$

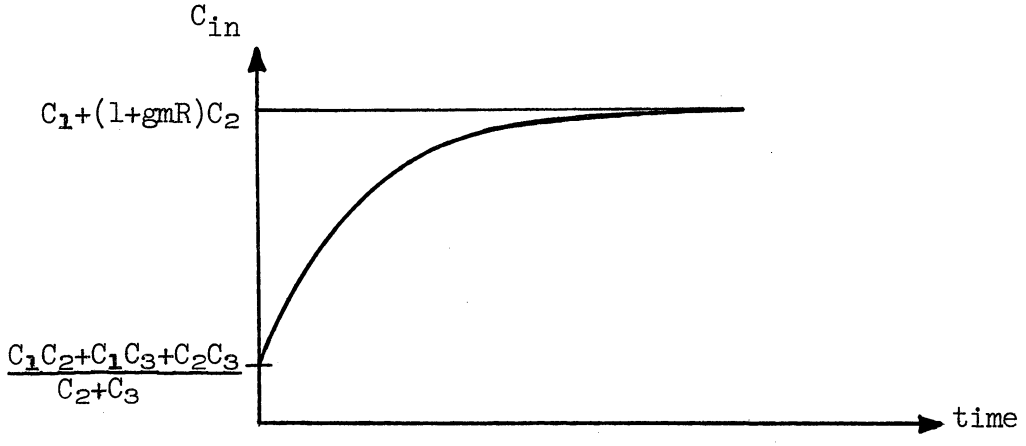

The input capacitance has reached 95% of its final value when $t = 3/\alpha$ or when

$$t = \frac{3\,R(C_1C_2 + C_1C_3 + C_2C_3)}{C_1 + (1 + g_mR)\,C_2} .$$

For the 437A triode with

$R = 1k,$
$C_1 = 11\ pF,$
$C_2 = 4\ pF,$ and
$C_3 = 1\ pF,$

t_c is calculated to be 0.89×10^{-9} sec.

That is, the input capacitance has reached 95% of $C_1 + (1 + gmR) C_2$ in a time of the order of 1 mμsec for the 437A. This means that for 10-mcps (or less) operation, the input capacitance may be considered to be just

$$Cin = C_1 + (1 + gm\ R)\ C_2.$$